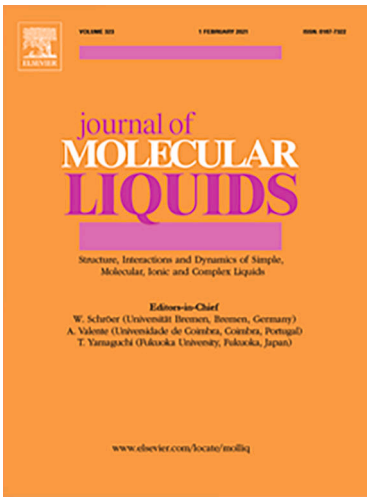

Measurements and predictions of densities and viscosities in CO_2 + hydrocarbon mixtures at high pressures and temperatures: CO_2 + *n*-pentane and CO_2 + *n*-hexane blends

Alejandro Moreau, Ilya Polishuk, José J. Segovia, Dirk Tuma, David Vega-Maza, M. Carmen Martín

PII: S0167-7322(22)01056-X
DOI: https://doi.org/10.1016/j.molliq.2022.119518
Reference: MOLLIQ 119518

To appear in: *Journal of Molecular Liquids*

Received Date: 8 February 2022
Revised Date: 26 April 2022
Accepted Date: 30 May 2022

Please cite this article as: A. Moreau, I. Polishuk, J.J. Segovia, D. Tuma, D. Vega-Maza, M. Carmen Martín, Measurements and predictions of densities and viscosities in CO_2 + hydrocarbon mixtures at high pressures and temperatures: CO_2 + *n*-pentane and CO_2 + *n*-hexane blends, *Journal of Molecular Liquids* (2022), doi: https://doi.org/10.1016/j.molliq.2022.119518

Measurements and predictions of densities and viscosities in CO_2 + hydrocarbon mixtures at high pressures and temperatures: CO_2 + *n*-pentane and CO_2 + *n*-hexane blends.

Alejandro Moreau[a], Ilya Polishuk[b], José J. Segovia[a], Dirk Tuma[c], David Vega-Maza[a], M. Carmen Martín[a,*]

[a] TermoCal Research Group, Research Institute on Bioeconomy, University of Valladolid, Paseo del Cauce 59, 47011 Valladolid, Spain.

[b] Department of Chemical Engineering, Ariel University, Ariel, 40700, Israel

[c] BAM Federal Institute for Materials Research and Testing, D-12200 Berlin, Germany

[*] corresponding author, e-mail: mcarmen.martin@eii.uva.es

Keywords: Carbon dioxide; *n*-alkanes; *n*-pentane; *n*-hexane; density; viscosity; predictive modelling

Abstract

This work reports new experimental data on densities and viscosities of (CO_2 + *n*-pentane) and (CO_2 + *n*-hexane) mixtures at high pressures and temperatures. The densities were measured by vibrating-tube densimeter with an expanded uncertainty (k = 2) smaller than 1.8 kg·m^{-3} at six isotherms (from 273.15 K to 373.15 K), twelve pressures starting at 5 MPa up to 100 MPa, and at six CO_2 molar compositions (from 0 to 0.6). The viscosities were measured by vibrating-wire viscometer with the corresponding relative expanded uncertainty (k = 2) smaller than 0.016 at five isotherms (from 273.15 K to 373.15 K), twelve pressures (from 5 MPa up to 100 MPa), and at two CO_2 molar compositions (0.1 and 0.3). The densities were fitted by the semiempirical Tammann-Tait equation for densities data and the Vogel-Fulcher-Tammann (VFT) equation for viscosity data, respectively. The Groupe Européen de Recherches Gazières (GERG-2008) equation of state was also applied for modelling the densities. Over-all robustness and reliability

of the Perturbed-Chain Statistical Association Fluid Theory (PC-SAFT) and its critical point-based modification (CP-PC-SAFT) were examined. Accuracies the Modified Yarranton-Satyro (MYS) coupled with CP-PC-SAFT and the NIST Reference Fluid Thermodynamic and Transport Properties Database (REFPROP 10) in predicting the viscosities were evaluated.

1. Introduction

Methods of crude oil extraction can be categorized in three different stages, namely primary, secondary, and tertiary techniques. Primary oil recovery processes are limited to natural rise of hydrocarbons from the bottom of the wellbore to the surface, combined with artificial lift techniques (such as the iconic pump jack). Extraction potential by this technique is limited, only around 10 % of the reservoir´s original oil in place can be extracted by this technique. Secondary recovery techniques prolong the productive life of an oil field by injection of water and gas to displace oil and drive it to the production wellbore, thus increasing oil recovery from 20 % up to 40 % of the original oil reservoir [1].

The ultimate way to increase oil production from an already depleted reservoir is using tertiary crude oil techniques or Enhanced Oil Recovery (EOR). This process uses heat, chemicals, or solvents and starts after primary and secondary techniques have already been deployed. The use of solvents, such as CO_2, is a specific EOR technique consisting in injecting CO_2 into the oil reservoir to improve recoverability, reducing its viscosity, swelling the crude oil, and decreasing the interfacial tension [2]. Although this method increases operation expenses, it is compensated with a yield of more than 60 % in oil recovery.

The main objective of EOR is the recovery of residual crude oil from a reservoir. However, nowadays, this technique qualifies for a second purpose, sequestration of CO_2 with a high potential in mitigation of global warming. Many oil reservoirs have the potential to sequester a great fraction of the injected CO_2 (around 40 % to 50 %) [3] injected and this procedure

generates a mixture of brine, crude oil, light hydrocarbons (natural gas liquid), and non-sequestered CO_2 stream. This CO_2 stream is treated and reinjected into the reservoir [4].

In that global scenario, the CO_2 sequestration process via EOR becomes an additional strategic technology to reduce world greenhouse gas emissions. By means of gas treatment technologies, such as carbon capture with aqueous solutions of amines, CO_2 can be captured from gas stream in natural gas processing, ammonia production, steel industry, or power plants.

For those reasons, knowledge of *pVT* behavior and transport properties of the mixtures (CO_2 + hydrocarbon) is mandatory for carrying out the EOR process at reservoir conditions. The first objective of this work is measuring densities and viscosities of (CO_2 + hydrocarbon) mixtures in wide ranges of pressures and temperatures, extending thus the previously reported data on densities of the binary CO_2 systems with the hydrocarbons *n*-decane, *n*-dodecane and squalene [5] to *n*-pentane and *n*-hexane. The range of measurements allows to extend the potential applications of the data since the techniques allow it.

There is still limited information on these systems in the literature. Regarding the (CO_2 + *n*-pentane) mixture, Besserer and Robinson [6] reported VLE at 277.7, 311.0, 344.2 and 377.6 K and the equilibrium-phase densities were calculated from the measured phase composition and refractive index by the Lorentz molar refractivity relationship. Kiran et al. [7] investigated the volumetric behavior of this system at pressures up to 70 MPa, five isotherms between 323 K and 423 K, and over the entire composition range including the pure compounds; they have assigned an uncertainty of 1.2 % to their measurements. Chen et al. [8] measured phase behavior and density at saturation conditions with an accuracy better than 1 $kg \cdot m^{-3}$, these measurements range from 312.35 K to 328.15 K and pressures up to 15 MPa. No viscosity data have been reported for this mixture so far.

As for the (CO_2 + *n*-hexane) mixture, Kaminishi et al. [9] measured vapor pressures and liquid densities at 273.15, 283.15, 298.15, and 303.15 K over the entire composition range with an

accuracy of 0.3 %. Tolley et al. [10] measured densities at 308.15 and 313.15 K, at pressures from 6 MPa to 12.5 MPa, and covering the entire composition range with an uncertainty of 1 kg m^{-3}. Wang et al. [11] reported density at the dew point at 50, 55, and 60 °C. Finally, Kian and Scurto [12] measured viscosity of compressed CO_2-saturated *n*-hexane at 25, 40, and 55 °C and pressures up to 107 bar with a standard uncertainty of less than 1 %.

The measurements performed in this work will contribute to consolidating the data inventory of these two mixtures. The new data also provide an excellent opportunity to examine an overall robustness and reliability of thermodynamic models, which is the second objective of this study.

2. Experimental

2.1. Materials

The two hydrocarbons were purchased from Sigma-Aldrich and Fluka Chemicals with the highest purity available, and CO_2 was supplied by Carburos Metálicos, Premier Líquido series. Their characteristics are summarized in Table 1. Purities were specified by the supplier and no further purification was carried out prior to investigation in the laboratory. However, the purities of the hydrocarbons were checked by gas chromatography (GC).

Table 1. Material description.

Compound	Source	CAS number	Mass fraction purity	Mass water content	Purification method
n-Pentane	Fluka Chemicals	109-66-0	≥ 0.99[a]	–	None
n-Hexane	Sigma-Aldrich	110-54-3	≥ 0.99[a]	–	None
CO_2	Carburos Metálicos	124-38-9	≥ 0.99995	< 7 ppm	None

[a] as stated by the supplier from GC analysis

2.2. Apparatus and procedure

2.2.1. Density measurements

Densities were measured using a vibrating-tube densimeter (Anton Paar DMA HPM, Anton Paar Spain S.L.U., Madrid). Pure water and vacuum were the calibration media for this study and details of the calibration procedure are reported in a previous paper [13]. This technique is able to measure density in the range of (0 to 3000) $kg \cdot m^{-3}$ with a resolution of 10^{-2} $kg \cdot m^{-3}$. The apparatus is fully automated using the Agilent VEE Pro software as a control system and for data acquisition [14]. The density of pentane and hexane was measured to check the performance of the technique. The densimeter can be operated either with liquid mixtures (prepared by weighing and charged manually into the system) or with mixtures where one component is maintained in liquid phase using a modification of the injection system. The complete modification of the apparatus is described by Zambrano et al. [5]. The experimental uncertainties were determined according to the recommendations in the GUM [15], whose details can be found in [13]. The resulting expanded uncertainty ($k = 2$) is less than 1.8 $kg \cdot m^{-3}$. Temperature was measured by means of an ASL-F100 thermometer with two resistant sensors (Pt100), whereas pressure was determined using a digital manometer (Druck DPI 104, General Electric). Both devices were calibrated in the laboratory being traceable to national standards. The corresponding expanded uncertainties ($k = 2$) are $U(T) = 20$ mK and $U_r(p) = 0.0002$.

2.2.2. Viscosity measurements

A vibrating-wire viscometer, developed in TermoCal laboratory, was used to accurately measure dynamic viscosities up to a maximum value of 35 mPa·s, at working temperatures from 288.15 K to 423.15 K and pressures up to 140 MPa. Details of this technique are reported in the previous works [16–18]. Our technique uses a gold-plated tungsten wire (length 50 mm and nominal radius 75 μm) anchored at both ends [19,20] as a sensor (provided by Prof. Trusler

from Imperial College London) and placed inside a pressure vessel, with an external constant magnetic field. The pressure vessel was immersed in a high-precision thermostatic bath and the fluid temperature is measured using two calibrated platinum resistance thermometers (PRT) with a standard uncertainty of 0.01 K. A Druck DPI 104 transducer records the pressure with an expanded uncertainty (k = 2) of 0.0002. Both devices were calibrated at the TermoCal laboratory using traceable standards to the Spanish National Metrology Institute (CEM) primary standards. The radius of the tungsten wire was calibrated using toluene as reference fluid and the accuracy of the viscosity measurements was first checked with dodecane.

In order to measure (CO_2 + hydrocarbon) mixtures, it was necessary to modify the injection system in the same way as for the densimeter [5]. The new scheme of the experimental vibrating-wire viscometer that was operated in this work is shown in Figure 1.

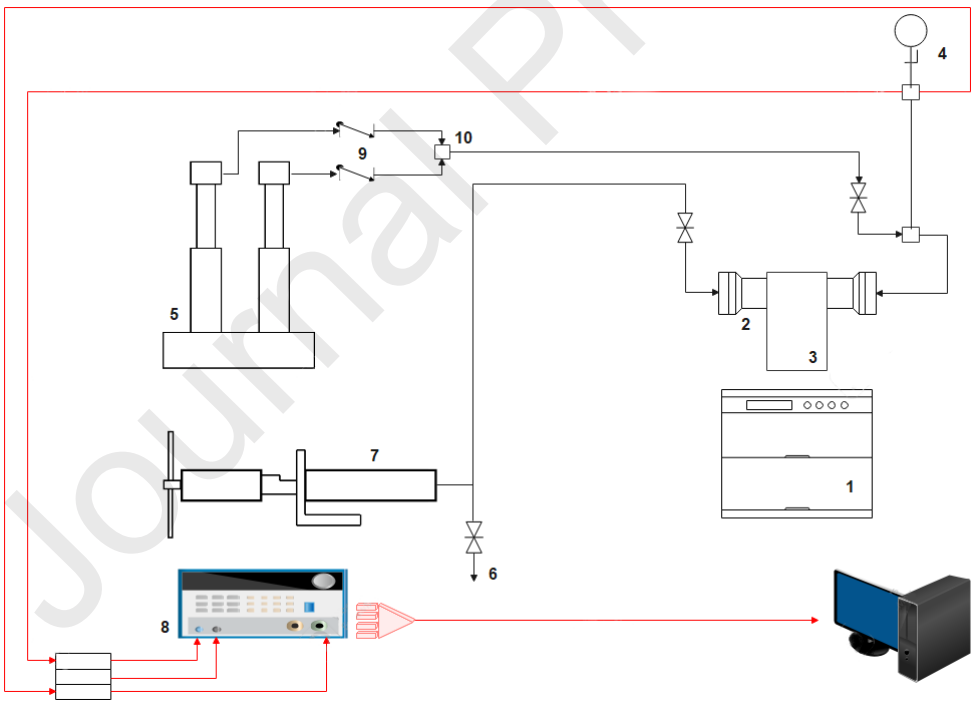

Figure 1. View of the experimental vibrating-wire rig: (1) thermostatic bath, (2) pressure vessel with the vibrating-wire sensor, (3) magnet, (4) pressure transducer, (5) ISCO syringe pumps, (6) Mity Mite valve (pressure controller), (7) pressure generator (a manually operated spindle

press), (8) lock-in amplifier, (9) check valves and (10) mixing point. The modification of the apparatus is mainly in the pressure line with the addition of the back-pressure system.

Two jacked injection pumps (ISCO Model 260D, Teledyne ISCO, Lincoln NE) were used to charge each pure component (hydrocarbon or CO_2). These pumps are connected by stainless steel pipes and valves to the pressure vessel, where the vibrating-wire sensor is located. The pressure control is performed using a pressure generator (HIP model 68-5.75-10, High Pressure Equipment Company, Erie PA) and a back-pressure valve (Mity Mite S-91XW, Equilibar, LLC, Fletcher NC).

The mixtures were prepared from known flow rates of each (pure) component, that are controlled and determined by the operating software of the injection pumps, and density of the pure compounds at the injection temperature and pressure. Densities for the pure hydrocarbons and CO_2 were obtained from the NIST Reference Fluid Thermodynamic and Transport Properties Database (REFPROP 10) [21] software with the corresponding reference for *n*-hexane [22], *n*-pentane [23], and CO_2 [24]. The molar flow rate is determined using Eq. (1):

$$n_i = \frac{Q_i \cdot \rho_i}{M_i} \qquad (1)$$

where for each component "*i*", n_i is the molar flow, Q_i is the volumetric flow given by the injection pump, ρ_i is the density at the injection conditions, and M_i is the molar mass.

The same filling procedure of preparing the densimeter was implemented for the viscometer. One of the dual ISCO pumps was filled with pure hydrocarbon at 6 MPa and 313.15 K and the second pump is loaded with CO_2 at the same pressure and 283.15 K assuring liquid phase. The targeted compositions were prepared by varying the flow rate of each pump, maintaining constant pressure with the back-pressure valve. The composition uncertainty depends on the quantity of each component and was reported by Zambrano et al. [5]. In the set-up of this

technique [16], the main contribution to the uncertainty budget was identified as the determination of the radius of the tungsten wire. The overall uncertainties of the viscosity measurements were recalculated considering the contribution of the mixture composition to the uncertainty at the most unfavorable case (i.e., CO_2 (1) + *n*-pentane (2) at the lowest temperature of 293.15 K). This procedure resulted in an increase of 0.1 % in the global uncertainty budget. The relative expanded uncertainty of these viscosity measurements is estimated better than 0.016 for a coverage factor $k = 2$ at all the investigated conditions.

3. Results and discussion

3.1 Density measurements

Experimental density measurements of two binary systems, (CO_2 (1) + *n*-pentane (2)) and (CO_2 (1) + *n*-hexane (2)) and the two pure hydrocarbons (*n*-pentane and *n*-hexane) were obtained at twelve different pressures, starting at 5 MPa up to 100 MPa and at six temperatures ranging from 273.15 K to 373.15 K. Both binary systems were measured at five molar compositions (x_1 = 0.1, 0.2, 0.3, 0.4, and 0.6). These experimental results are presented in Table 2 and Table 3, respectively.

Table 2. Experimental densities ρ for (CO_2 (1) + *n*-pentane (2)) mixtures at different conditions of temperature T, pressure p, and CO_2 molar concentration x_1. [a]

ρ / kg·m^{-3}						
	T / K					
p / MPa	273.15 $x_1 = 0$	293.15	313.15	333.15	353.15	373.15
1.00	646.6	627.4	607.5	586.4	563.7	538.9
5.00	650.6	632.3	613.3	593.5	572.5	550.2
10.00	655.3	637.7	619.7	601.2	581.8	561.6

15.00	659.7	642.7	625.5	608.0	589.8	571.2
20.00	663.8	647.4	630.9	614.2	597.0	579.5
30.00	671.4	656.0	640.6	625.1	609.4	593.8
40.00	678.2	663.6	649.2	634.7	620.1	605.7
50.00	684.6	670.6	656.8	643.2	629.5	615.9
60.00	690.4	677.0	663.8	650.9	637.8	625.0
70.00	695.9	683.0	670.3	657.9	645.4	633.2
80.00	701.1	688.6	676.3	664.4	652.4	640.6
90.00	706.0	693.8	682.0	670.4	658.8	647.5
100.00	710.5	698.7	687.2	676.0	664.8	653.9
	$x_1 = 0.1000 \pm 0.0017$					
5.00	660.3	640.5	619.8	598.2	575.2	550.2
10.00	665.3	646.5	627.1	607.0	586.1	564.0
15.00	670.1	652.0	633.5	614.6	595.4	575.2
20.00	674.5	657.1	639.4	621.5	603.6	584.9
30.00	682.6	666.4	650.0	633.7	618.0	601.4
40.00	690.0	674.6	659.2	644.5	630.5	615.3
50.00	696.8	682.1	667.6	654.2	641.4	627.4
60.00	703.0	688.9	675.4	663.0	651.2	638.2
70.00	708.8	695.3	682.7	671.1	660.1	647.8
80.00	714.3	701.2	689.5	678.6	668.2	656.7
90.00	719.4	706.8	696.0	685.6	675.8	664.6
100.00	724.3	712.1	702.0	692.1	682.7	672.1
	$x_1 = 0.2000 \pm 0.0021$					
5.00	674.4	652.5	629.3	604.5	577.7	547.8
10.00	680.3	659.5	637.7	615.0	591.1	565.5
15.00	685.6	665.7	645.1	624.1	602.2	579.3

20.00	690.6	671.5	651.9	632.0	611.8	590.8
30.00	699.6	681.9	663.8	645.8	628.1	609.8
40.00	707.8	691.0	674.1	657.8	642.0	625.4
50.00	715.2	699.2	683.3	668.4	654.0	638.8
60.00	722.0	706.8	691.8	677.9	664.7	650.6
70.00	728.4	713.7	699.6	686.6	674.3	661.1
80.00	734.2	720.1	706.9	694.6	683.1	670.6
90.00	739.8	726.2	713.7	702.0	691.1	679.2
100.00	745.1	731.9	720.1	708.9	698.6	687.2
	$x_1 = 0.3002 \pm 0.0026$					
5.00	688.8	664.2	637.9	609.4	577.5	
10.00	695.4	672.3	647.9	622.2	594.6	564.7
15.00	701.4	679.4	656.6	632.9	608.0	581.8
20.00	707.0	686.0	664.3	642.2	619.3	595.6
30.00	717.0	697.5	677.7	657.9	637.6	617.1
40.00	725.9	707.6	689.3	671.0	652.5	634.1
50.00	734.1	716.7	699.4	682.4	665.3	648.2
60.00	741.4	724.9	708.6	692.6	676.4	660.4
70.00	748.3	732.5	716.9	701.7	686.4	671.2
80.00	754.7	739.5	724.6	710.1	695.4	680.9
90.00	760.8	746.0	731.9	717.9	703.7	689.7
100.00	766.4	752.2	738.5	725.0	711.4	697.8
	$x_1 = 0.3999 \pm 0.0029$					
5.00	705.9	677.6	646.9	612.8		
10.00	713.3	687.1	659.2	629.3	596.6	559.9
15.00	720.2	695.4	669.5	642.5	613.6	582.9
20.00	726.5	703.0	678.6	653.6	627.3	600.2

30.00	737.8	716.1	694.1	671.8	649.1	626.0
40.00	747.7	727.5	707.1	686.8	666.1	645.4
50.00	756.7	737.6	718.5	699.5	680.3	661.1
60.00	764.9	746.7	728.6	710.7	692.5	674.6
70.00	772.4	755.0	737.7	720.6	703.4	686.4
80.00	779.5	762.7	746.1	729.6	713.2	697.1
90.00	786.0	769.8	753.8	737.9	722.1	706.7
100.00	792.1	776.5	760.9	745.6	730.4	715.6
	$x_1 = 0.5999 \pm 0.0028$					
5.00	750.0	709.8	662.9			
10.00	760.8	724.5	684.4	639.0	584.2	
15.00	770.3	736.8	700.9	662.0	619.1	571.5
20.00	778.9	747.5	714.5	679.8	642.7	603.4
30.00	793.8	765.5	736.5	706.8	675.6	644.5
40.00	806.7	780.6	754.1	727.5	699.4	672.2
50.00	818.2	793.6	769.0	744.4	718.7	693.6
60.00	828.4	805.3	782.0	758.8	734.9	711.6
70.00	837.9	815.7	793.5	771.4	749.1	727.0
80.00	846.5	825.3	803.9	782.8	761.7	740.6
90.00	854.6	834.0	813.5	793.2	773.1	752.9
100.00	862.1	842.2	822.4	802.7	783.5	763.9

[a] Expanded uncertainties ($k = 2$): $U(T) = 0.02$ K; $U_r(p) = 0.0002$; and $U(\rho) = 1.8$ kg·m^{-3}.

Table 3. Experimental densities ρ for (CO_2 (1) *n*-hexane (2)) mixtures at different conditions of temperature T, pressure p, and CO_2 molar concentration x_1. [a]

ρ / kg·m^{-3}

	T / K					
p / MPa	273.15	293.15	313.15	333.15	353.15	373.15
	$x_1 = 0$					
1.00	678.5	661.0	642.8	623.9	604.1	583.3
5.00	682.0	665.1	647.6	629.6	611.0	591.5
10.00	686.2	669.8	653.0	636.0	618.5	600.4
15.00	690.1	674.2	658.0	641.8	625.2	608.3
20.00	693.7	678.4	662.8	647.2	631.3	615.2
30.00	700.6	686.1	671.3	656.7	642.1	627.4
40.00	706.9	693.0	679.1	665.3	651.6	637.9
50.00	712.8	699.4	686.1	673.0	660.0	647.0
60.00	718.2	705.4	692.6	680.1	667.6	655.3
70.00	723.3	711.0	698.6	686.5	674.6	662.8
80.00	728.2	716.2	704.2	692.6	681.1	669.8
90.00	732.8	721.2	709.5	698.2	687.1	676.2
100.00	737.1	725.7	714.5	703.5	692.7	682.1
	$x_1 = 0.1002 \pm 0.0017$					
5.00	691.0	672.7	653.8	634.3	613.9	592.4
10.00	695.6	678.0	660.0	641.6	622.6	602.9
15.00	699.8	682.8	665.5	648.1	630.2	611.9
20.00	703.8	687.4	670.7	654.0	637.1	619.9
30.00	711.2	695.7	680.1	664.6	649.4	633.8
40.00	718.0	703.2	688.4	674.0	660.2	645.8
50.00	724.2	710.0	696.0	682.6	669.9	656.5
60.00	730.0	716.4	703.0	690.6	678.7	666.1
70.00	735.5	722.3	709.7	698.0	686.9	674.9
80.00	740.6	727.9	715.9	704.9	694.4	683.0

90.00	745.5	733.1	721.8	711.4	701.4	690.4
100.00	750.1	738.1	727.5	717.5	707.9	697.4
	$x_1 = 0.2000 \pm 0.0021$					
5.00	701.8	681.7	661.0	639.3	616.5	592.0
10.00	706.8	687.7	668.0	647.7	626.7	604.6
15.00	711.4	693.1	674.2	655.1	635.4	615.2
20.00	715.8	698.1	680.0	661.8	643.2	624.3
30.00	723.8	707.2	690.4	673.6	656.7	639.7
40.00	731.2	715.4	699.5	683.9	668.3	652.6
50.00	737.9	722.8	707.8	693.1	678.5	663.9
60.00	744.1	729.7	715.3	701.4	687.7	674.0
70.00	750.0	736.1	722.3	709.1	696.2	683.1
80.00	755.5	742.0	728.8	716.2	704.0	691.4
90.00	760.7	747.6	735.0	722.9	711.1	699.1
100.00	765.6	752.9	740.7	729.2	717.8	706.2
	$x_1 = 0.2999 \pm 0.0026$					
5.00	713.5	691.5	668.5	644.2	618.1	589.5
10.00	719.1	698.2	676.5	654.1	630.4	605.4
15.00	724.2	704.2	683.6	662.6	640.8	618.0
20.00	729.1	709.8	690.2	670.2	649.7	628.7
30.00	737.9	719.9	701.7	683.5	665.0	646.4
40.00	745.9	728.8	711.8	694.9	677.8	660.9
50.00	753.2	737.0	720.8	704.8	689.0	673.3
60.00	759.9	744.4	729.0	713.8	698.9	684.3
70.00	766.2	751.3	736.5	722.0	708.1	694.3
80.00	772.1	757.7	743.4	729.5	716.4	703.4
90.00	777.7	763.7	749.9	736.6	724.1	711.6

100.00	783.0	769.3	755.9	743.1	731.3	719.3
	$x_1 = 0.4000 \pm 0.0029$					
5.00	728.0	703.2	676.7	648.4	617.1	
10.00	734.4	711.0	686.4	660.6	633.1	600.7
15.00	740.3	717.9	694.7	670.9	645.9	619.6
20.00	745.7	724.3	702.3	679.9	656.7	633.7
30.00	755.6	735.7	715.5	695.2	674.7	655.6
40.00	764.4	745.7	726.8	708.2	689.6	672.5
50.00	772.5	754.7	736.9	719.6	702.5	686.5
60.00	779.9	762.9	746.0	729.7	713.9	698.7
70.00	786.8	770.4	754.3	739.0	724.2	709.5
80.00	793.2	777.5	762.0	747.5	733.5	719.3
90.00	799.2	784.0	769.2	755.4	742.0	728.1
100.00	804.9	790.2	776.0	762.7	750.0	736.4
	$x_1 = 0.5999 \pm 0.0028$					
5.00	766.8	732.1				
10.00	775.7	743.9	709.3	671.3	628.0	
15.00	783.9	754.0	722.3	688.6	652.2	612.7
20.00	791.2	763.0	733.4	702.7	670.4	636.2
30.00	804.4	778.5	752.1	725.2	697.6	669.6
40.00	815.8	791.8	767.5	743.1	718.3	693.7
50.00	826.1	803.5	780.7	758.1	735.3	713.0
60.00	835.4	814.0	792.3	771.1	749.7	729.3
70.00	844.0	823.4	802.8	782.6	762.5	743.5
80.00	852.0	832.2	812.2	792.9	774.0	756.1
90.00	859.4	840.2	820.9	802.4	784.4	767.5
100.00	866.4	847.8	829.0	811.1	794.0	777.9

[a] Expanded uncertainties ($k = 2$): $U(T) = 0.02$ K; $U_r(p) = 0.0002$; and $U(\rho) = 1.8$ kg·m^{-3}.

As can be seen from the experimental data, $\rho_{(CO2 + n\text{-hexane})} > \rho_{(CO2 + n\text{-pentane})}$ at the same conditions of pressures, temperatures, and composition. As expected, the density monotonically increases with pressure and decreases with temperature for all binary systems investigated. This phenomenon becomes more pronounced at higher CO_2 mole fractions.

As regards the effect of increasing pressure, the minimum density increase, observed for a change in pressure from 10 MPa to 100 MPa, is 8 % for the system (CO_2 + *n*-hexane) and 9 % for (CO_2 + *n*-pentane), being both at the lowest temperature (T = 273.15 K) and composition ($x_1 = 0.1$). In the case of the pure hydrocarbons the corresponding density increase amounts to 7 % and 8 %, respectively. The maximum density increase is shown at the highest temperature (373.15 K) and composition ($x_1 = 0.6$). Density in the system (CO_2 + *n*-hexane) grows by 27 % from 15 MPa to 100 MPa at 373.15 K and by 34 % for the system with (CO_2 + *n*-pentane) at the same conditions.

Expectedly, densities decrease with increasing temperature. In the range from 273.15 K to 373.15 K, a minimum decrease of 7 % is obtained for both binary systems at 100 MPa and x_1 = 0.1. The corresponding density drop for the pure hydrocarbons is 7 % for *n*-hexane and 8 % for *n*-pentane, respectively. The maximum decrease is always observed at the lowest pressure measured (at 15 MPa and $x_1 = 0.6$ in our case), the lowering in density is by 22 % for the mixture with *n*-hexane and by 26 % for the mixture with *n*-pentane.

The addition of CO_2 to the hydrocarbon increases the density of the system compared with the pure hydrocarbon up to 18 % for *n*-hexane and 21 % for *n*-pentane at 100 MPa, 273.15 K, and $x_1 = 0.6$. In general, the densities monotonically increase when the CO_2 content is increased, however, a few exceptions were found: in the (CO_2 + *n*-pentane) mixture at the p, T-coordinate (353.15 K, 10 MPa) when the composition changes from $x_1 = 0.3$ to $x_1 = 0.4$ and at (373.15 K,

15 MPa) when the composition changes from $x_1 = 0.4$ to $x_1 = 0.6$. For the (CO_2 + *n*-hexane) system, when the composition changes from $x_1 = 0.3$ to $x_1 = 0.4$ at (353.15 K, 5 MPa) and (373.15 K, 10 MPa) and also when the composition changes from $x_1 = 0.4$ to $x_1 = 0.6$ at (353.15 K, 10 MPa) and (373.15 K, 15 MPa). This particular behavior was also observed for the mixture (CO_2 + *n*-pentane) by Kiran et al. [7]. They explain that phenomenon with "a crossover region when the density for mixtures with high carbon dioxide content becomes lower than the density for mixtures with lower carbon dioxide content". In Figures 2 and 3, the behavior of density as function of pressure at constant temperature is displayed for the five compositions investigated including the pure hydrocarbons.

a)

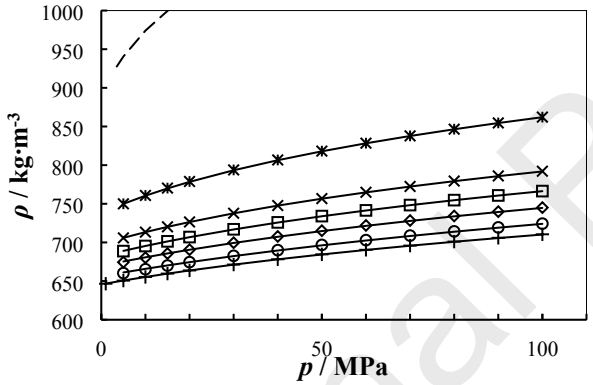

b)

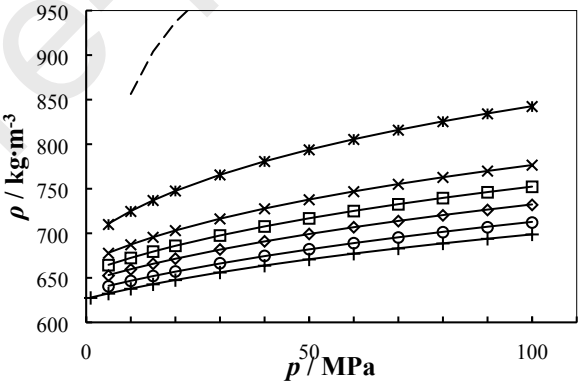

c)

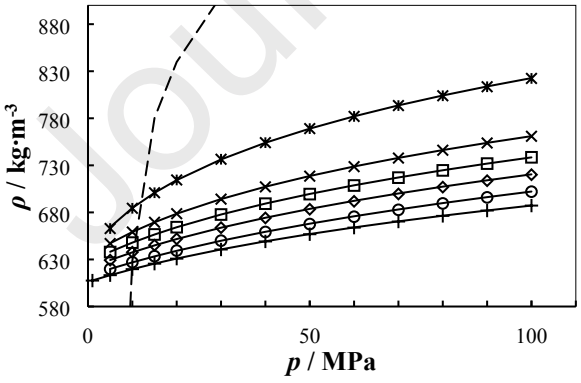

d)

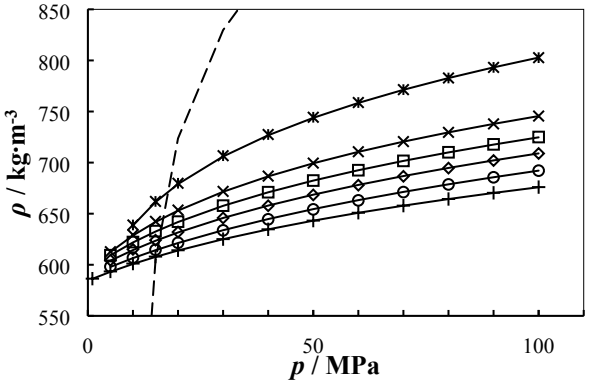

e)

f)

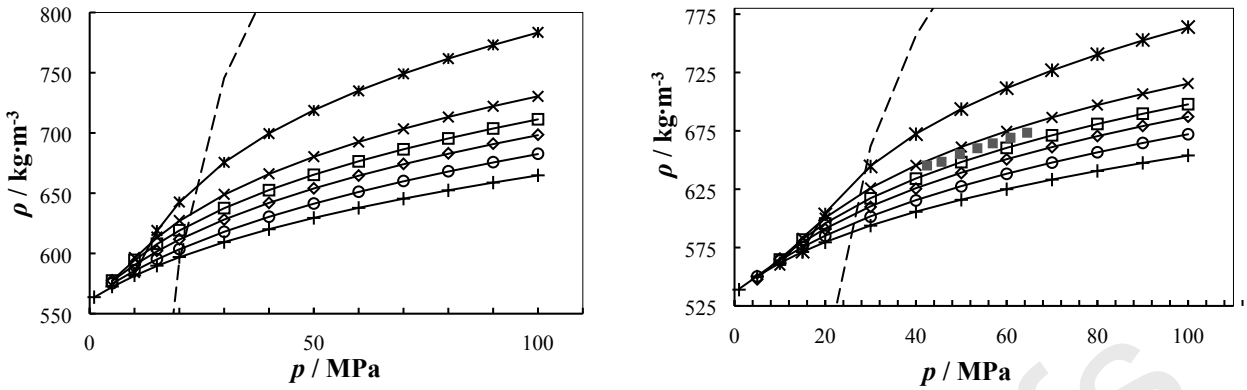

Figure 2. Experimental density of the system (CO_2 (1) + *n*-pentane (2)) as function of pressure, at temperatures: (a) 273.15 K; (b) 293.15 K; (c) 313.15 K; (d) 333.15 K; (e) 353.15 K; (f) 373.15 K and different compositions: (+) $x_{CO2} = 0$; (○) $x_1 = 0.1$; (◊) $x_1 = 0.2$; (○) $x_1 = 0.3$; (×) $x_1 = 0.4$; (~~×~~) $x_1 = 0.6$. Lines represent the calculated values using a modified Tammann-Tait equation with the corresponding parameters given in Table 4. The dashed lines (----) represent pure CO_2 [24]. In f) experimental data of Kiran et al. [7] at $x_1 \sim 0.3$ are represented using filled grey symbols.

a) b)

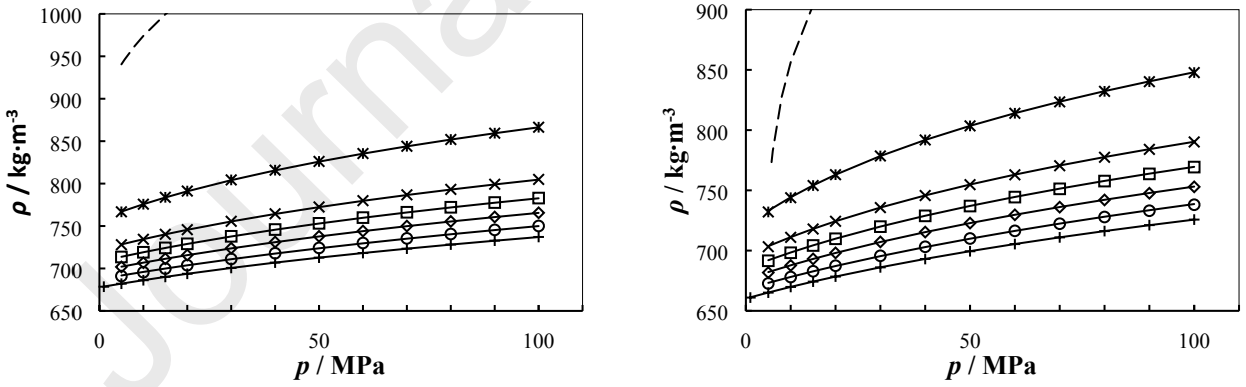

c) d)

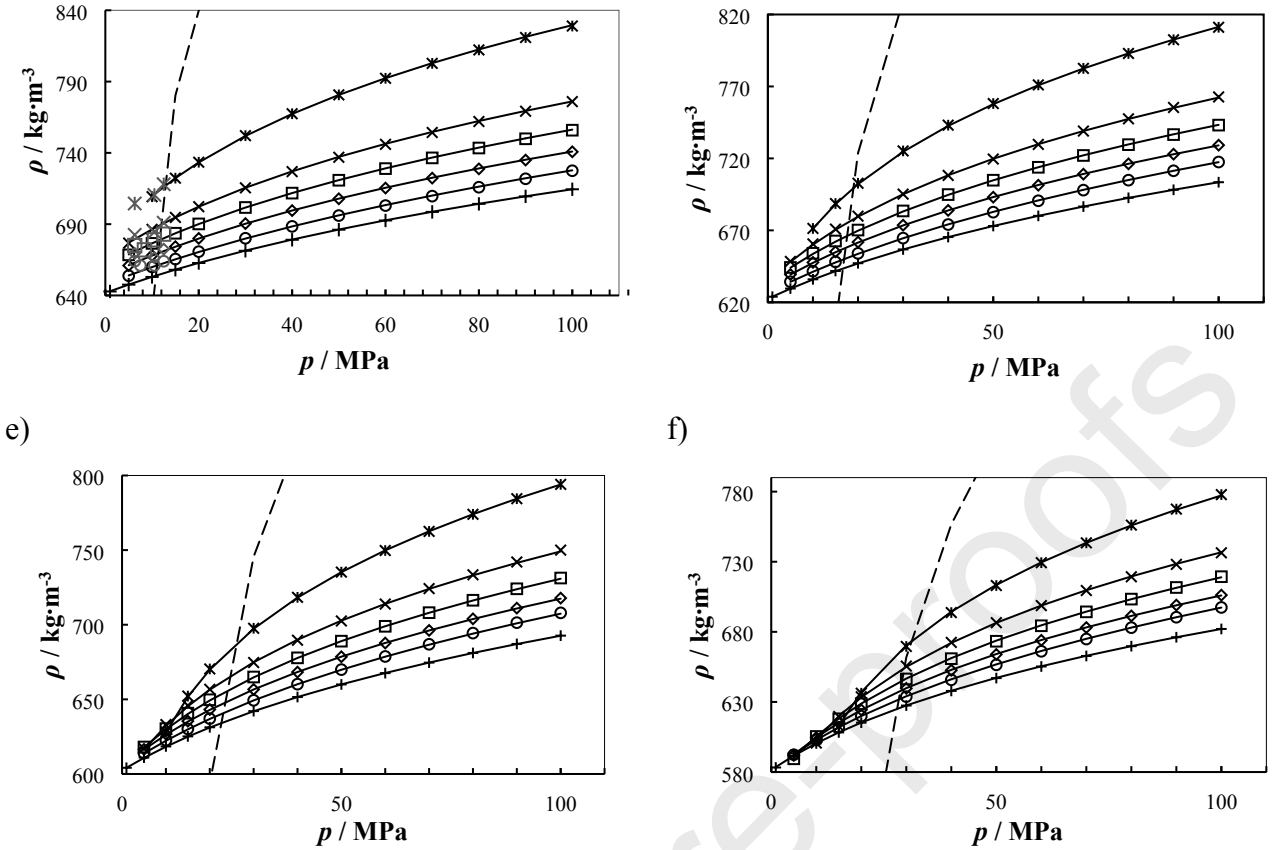

Figure 3. Experimental density of the system (CO_2 (1) + *n*-hexane (2)) as function of pressure, temperatures: (a) 273.15 K; (b) 293.15 K; (c) 313.15 K; (d) 333.15 K; (e) 353.15 K; (f) 373.15 K and at different compositions: (+) $x_1 = 0$; (○) $x_1 = 0.1$; (◊) $x_1 = 0.2$; (□) $x_1 = 0.3$; (×) $x_1 = 0.4$; (✱) $x_1 = 0.6$. Lines represent the calculated values using a modified Tammann-Tait equation with the corresponding parameters given in Table 4. The dashed lines (----) represent pure CO_2 [24]. In c) experimental data of Tolley et al. [10] are represented using grey symbols.

The experimental data were correlated by a modified Tammann-Tait equation (Eq. (2)) for each individual composition:

$$\rho(T,p) = \frac{A_0 + A_1 T + A_2 T^2}{1 - C\ln\left(\dfrac{B_0 + B_1 T + B_2 T^2 + p}{B_0 + B_1 T + B_2 T^2 + p_{\mathrm{ref}}}\right)} \qquad (2)$$

The fitting results are shown in Table 4, which contains the adjustable parameters and the standard deviation of the adjustment (σ) according to Eq. 3. A statistical analysis was executed

using both experimental and calculated data (calculated by Eq. 2) to evaluate the performance of this model: *AAD* (Average Absolute Deviation (Eq. 4)); *BIAS* (mean deviation (Eq. 5)); *MAD* (Maximum Absolute Deviation (Eq. 6)) and *RMS* (Root Mean Square (Eq. 7)).

$$\sigma = \sqrt{\frac{\sum_i (Calculated_i - Experimental_i)^2}{N - N_p}} \qquad (3)$$

$$AAD\ /\ \% = \frac{1}{N}\sum_i \left| 100 \cdot \frac{Calculated_i - Experimental_i}{Experimental_i} \right| \qquad (4)$$

$$BIAS\ /\ \% = \frac{1}{N}\sum_i 100 \cdot \frac{Calculated_i - Experimental_i}{Experimental_i} \qquad (5)$$

$$RMS\ /\ \% = \sqrt{\frac{1}{N}\sum_i \left(100 \cdot \frac{Calculated_i - Experimental_i}{Calculated_i} \right)^2 - BIAS^2} \qquad (6)$$

In Equations (3 to 6), N is the number of experimental points and N_p is the number of parameters.

$$MAD\ /\ \% = \max \left| 100 \cdot \frac{Calculated_i - Experimental_i}{Experimental_i} \right| \qquad (7)$$

Table 4. Fitting parameters of Eq. (2), standard deviations σ, average absolute deviation *AAD*, and maximum absolute deviations *MAD* for the density measurements.

CO_2 (1) + *n*-pentane (2)						
x_1	0	0.1	0.2	0.3	0.4	0.6
A_0 / kg·m^{-3}	779.254	836.797	820.179	856.865	839.221	888.085
A_1 / kg·m^{-3}·K^{-1}	–0.05534	–0.30589	0.00953	–0.07009	0.31865	0.69476
A_2 / kg·m^{-3}·K^{-2}	–0.00157	–0.00123	–0.00198	–0.00191	–0.00285	–0.00413
B_0 / MPa	330.679	454.708	405.808	331.151	318.211	312.873
B_1 / MPa·K^{-1}	–1.4406	–2.1103	–1.8996	–1.5329	–1.5165	–1.5645

B_2 / MPa·K^{-2}	0.00159	0.00249	0.00224	0.00176	0.00178	0.00189
C	0.08884	0.10034	0.09694	0.09374	0.09194	0.09560
σ / kg·m^{-3}	0.20	0.35	0.40	0.20	0.30	0.30
AAD / %	0.02	0.04	0.05	0.02	0.03	0.05
MAD / %	0.12	0.13	0.14	0.07	0.15	0.23
RMS / %	0.03	0.05	0.06	0.03	0.05	0.07
p_{ref} / MPa	1	5	5	10	10	15
CO_2 (1) + *n*-hexane (2)						
x_1	0	0.1	0.2	0.3	0.4	0.6
A_0 / kg·m^{-3}	840.607	881.311	874.863	861.582	903.506	955.208
A_1 / kg·m^{-3}·K^{-1}	–0.33061	–0.47707	–0.29274	–0.03279	–0.10933	0.16167
A_2 / kg·m^{-3}·K^{-2}	–0.00096	–0.00079	–0.00124	–0.00186	–0.00187	–0.00289
B_0 / MPa	339.146	445.716	369.062	345.036	341.448	320.514
B_1 / MPa·K^{-1}	–1.3995	–1.9595	–1.6173	–1.5313	–1.5532	–1.5352
B_2 / MPa·K^{-2}	0.00148	0.00221	0.00180	0.00170	0.00174	0.00178
C	0.08837	0.09936	0.09313	0.09160	0.09238	0.09465
σ / kg·m^{-3}	0.10	0.20	0.27	0.44	0.36	0.49
AAD / %	0.01	0.03	0.02	0.03	0.04	0.03
MAD / %	0.05	0.10	0.07	0.12	0.38	0.14
RMS / %	0.03	0.04	0.03	0.04	0.06	0.06
p_{ref} / MPa	1	5	5	5	10	15

According to Table 4, the modified Tammann-Tait equation is capable to fit the density data with standard deviations below the experimental uncertainty.

Unfortunately, not all the previously data can be directly compared with the current results. In particular, the data of Kiran et al. [7] are available for pure *n*-pentane nearly $x_1 = 0.3$ (20 % weight CO_2 reported in the article). Thus, these data were compared with the results of Tammann-Tait equation attached by parameters listed in Table 4. In the case of the pure *n*-pentane, the *AAD* from 30 experimental points at $T = 348$ K and 373 K is 0.55 %. In a case of the mixture, the *AAD* from 33 experimental points at $T = 323$ K, 348 K and 373 K is 0.79 %. These results remain within the reported uncertainty of literature data (1.2 %).

Audonnet and Pádua [25] also measured *n*-pentane density and viscosity in a similar temperature and pressure ranges (from 303 to 383 K up to 100 MPa), reporting 40 experimental points. The application of our Tammann-Tait fitting resulted in an *AAD* of 0.29 %, which is close to their assigned accuracy (0.2 %).

Furthermore, Tolley et al. [10] reported experimental densities for the binary system (CO_2 + *n*-hexane) up to 12.5 MPa and two temperatures of $T = 308.15$ K and 313.15 K at the compositions similar to the current ones. Application of the Tammann-Tait approach to these 38 experimental points yielded an *AAD* of 0.29 %, which is in agreement with the uncertainty of our measurements. In the case of pure *n*-hexane, the *AAD* was 0.12 %.

The *AAD* of Tammann-Tait equation from additional high pressure data of *n*-hexane are following: 0.07 % in the case of Regueira et al. [26], reporting 43 points up to 60 MPa from 278.15 K till 373.15 K, 0.09 % from the data of Zhou et al. [27], providing 30 points up to 40 MPa from 293.15 K till 313.15 K; 0.17 % from the data of Camacho-Camacho and Galicia-Luna [28], containing 153 points up to 25 MPa from 313 till 362 K.

Other literature data available for the binary systems (CO_2 (1) + *n*-pentane (2)) [8] and (CO_2 (1) + *n*-hexane (2)) [9] were reported at different compositions, which hinders the direct comparison with our measurements.

The current experimental data were used for testing three different equations-of-state (EoS) models, namely the Perturbed-Chain Statistical Association Fluid Theory (PC-SAFT) [29], its critical point-based revision (CP-PC-SAFT) [30] and the Groupe Européen de Recherches Gazières (GERG-2008) reference equation of state [31,32]. The latter model is a reference equation for gases covering 21 pure components, including *n*-pentane, *n*-hexane, and CO_2 and it is widely used in industrial applications. Unlike GERG-2008, the SAFT models are not restricted to specific compounds. The details of these approaches were discussed in their initial publications [29,30]. Obviously, the precision of SAFTs in modelling densities is inferior in comparison with the system and property-specific empirical models, such as the modified Tammann-Tait equation. However, their major advantage over correlation models is the universality and the applicability for simultaneous estimation of all thermodynamic properties. The molecular parameters of PC-SAFT are usually obtained by fitting the vapor pressures and saturated liquid densities of pure compounds. Evidently, consideration of different databases influences the resulting parameter values. Besides that, this model usually overestimates the pure compound critical temperatures and pressures. Unlike that, the parameters of CP-PC-SAFT are solved by a standardized numerical procedure at the pure compound points along with one coordinate at a low temperature, which typically is at the triple point. Consequently, this model rigorously obeys the pure-compound critical temperatures and pressures and thus requires a substantially smaller amount of input data. At the same time, there is a price to pay for this enhanced predictive character. In particular, CP-PC-SAFT often underestimates the vapor pressures away from the critical points.

So far it was found that an appropriate modelling of phase equilibria in (CO_2 + *n*-alkane) homologues series can be achieved by adopting a universal value of the binary parameter k_{12} = 0.12 for PC-SAFT [33,34] and k_{12} = 0.09 for CP-PC-SAFT [35]. Figures S1 and S2 of the Supplementary Material compare the performances of both approaches in modelling the

compositions of phase equilibria and the densities of saturated phases for the systems (CO_2 + n-C_nH_{2n+2}) with n = 5, 6, 7, 10, 14, and 18. It can be seen that in the cases of lighter members of the series (CO_2 + *n*-pentane, *n*-hexane, and *n*-heptane) the results of both approaches are rather similar. More significant differences between them can be observed for the system (CO_2 + *n*-decane). On the one hand, CP-PC-SAFT with the adopted k_{12} value erroneously estimates the liquid-liquid phase split at 310.9 K for this system, while PC-SAFT correctly predicts the topology of phase behavior [33]. On the other hand, CP-PC-SAFT is more accurate in modelling the bubble-point data. Figure S1 also demonstrates that this advantage of CP-PC-SAFT becomes more pronounced in the cases of heavier alkane homologues, such as (CO_2 + *n*-tetradecane and + *n*-octadecane).

Figure S3 of the Supplementary Material illustrates that both models under consideration truthfully predict the excess enthalpies of (CO_2 + *n*-alkanes), namely their positive values for the vapor phases and negative for the liquid phases, respectively. Some of these data are estimated more accurately by CP-PC-SAFT but other data by PC-SAFT.

Table S1 of the Supplementary Material summarizes the absolute average deviations (*AAD* / %) in predicting the high-pressure density and speed of sound data currently available for the (CO_2 + *n*-alkanes) series. In the investigated pressure range (up to 130 MPa) both models typically exhibit minor deviations from the density data. With the exception of (CO_2 + *n*-hexadecane), the deviations exhibited by PC-SAFT are smaller. However, CP-PC-SAFT most probably becomes superior at the higher pressures. This assumption can be supported by a clear advantage of this model in predicting the speed of sound data.

Table 5 lists the results of the statistical analysis of deviations of GERG-2008, PC-SAFT and CP-PC-SAFT from the current density data. Besides the *AAD* / %, it also provides the *BIAS* / %, root mean square (*RMS* / %) and maximum absolute deviation (*MAD* / %) values.

Table 5. Statistical analysis of deviations of GERG-2008, PC-SAFT, and CP-PC-SAFT from the experimental density data of this study.

CO_2 (1) + *n*-pentane (2)							
x_1		0	0.1	0.2	0.3	0.4	0.6
AAD / %	GERG-2008	0.06	0.4	0.5	1.0	1.4	2.1
	PC-SAFT	0.7	0.5	0.4	0.6	0.6	0.6
	CP-PC-SAFT	1.7	1.9	1.8	2.0	2.1	1.9
BIAS / %	GERG-2008	0.04	0.3	0.5	1.0	1.4	2.1
	PC-SAFT	–0.2	0.03	–0.05	0.2	0.3	0.3
	CP-PC-SAFT	1.7	1.9	1.8	2.0	2.1	1.7
RMS / %	GERG-2008	0.07	0.3	0.9	0.2	0.3	0.3
	PC-SAFT	0.8	0.6	0.5	0.6	0.7	0.7
	CP-PC-SAFT	1.1	1.4	1.4	1.4	1.5	1.5
MAD / %	GERG-2008	0.2	0.8	0.9	1.3	1.8	2.5
	PC-SAFT	1.5	1.0	1.1	1.4	1.6	1.8
	CP-PC-SAFT	2.2	2.7	2.5	2.7	2.8	2.7
CO_2 (1) + *n*-hexane (2)							
x_1		0	0.1	0.2	0.3	0.4	0.6
AAD / %	GERG-2008	0.05	2.9	5.9	8.7	11.4	15.0
	PC-SAFT	0.7	0.6	0.7	0.8	0.7	0.7
	CP-PC-SAFT	1.0	1.1	1.3	1.5	1.6	1.6
BIAS / %	GERG-2008	–0.02	2.9	5.9	8.7	11.4	15.0
	PC-SAFT	0.4	0.5	0.6	0.7	0.7	0.7
	CP-PC-SAFT	1.0	1.1	1.3	1.5	1.6	1.5

	GERG-2008	0.06	0.2	0.2	1.1	0.5	0.7
RMS / %	PC-SAFT	0.8	0.7	0.8	0.9	0.8	0.8
	CP-PC-SAFT	0.6	0.8	0.9	1.0	1.2	1.3
	GERG-2008	0.1	3.1	6.3	9.5	12.3	16.4
MAD / %	PC-SAFT	1.8	1.4	1.5	1.7	1.5	1.7
	CP-PC-SAFT	1.4	1.6	1.7	2.0	2.2	2.4

As seen, similarly to most other systems belonging to the (CO_2 + *n*-alkane) series, PC-SAFT predicts the current density data more accurately than CP-PC-SAFT. In the case of (CO_2 + *n*-pentane), all the considered models display a reasonably accurate performance. The *AAD* of GERG-2008 is smaller than that of both SAFT models at $x_1 = 0$ for the pure alkane and the low CO_2 content of $x_1 = 0.1$. However, at the higher concentrations of CO_2 PC-SAFT becomes superior. CP-PC-SAFT has a smaller *AAD* than GERG-2008 at $x_1 = 0.6$. At the same composition, CP-PC-SAFT exhibits the highest values of *MAD*.

It can also be seen that, in the case of the second system (CO_2 + *n*-hexane), GERG-2008 precisely estimates the densities of pure *n*-hexane which can be expected from the intentional application areas. However, the addition of CO_2 results in substantial deterioration of its performance. So, at $x_1 = 0.2$ and higher, the predictions of this model become particularly inaccurate, and at $x_1 = 0.6$ the *AAD* already amounts to 13.9 % and the *MAD* to 16.4 %, respectively. Unlike that, both SAFT approaches continue to yield reasonably good results in the entire composition range with an $AAD \leq 1.6$ % in the case of CP-PC-SAFT and ≤ 0.8 % of PC-SAFT. The corresponding *MAD* values also remain reasonable small. The poor performance of the GERG-2008 model can be explained by a lack of consolidated of (CO_2 + *n*-hexane) at the time of model build-up when only the VLE data were used for fitting the parameters for this system [31]. This result emphasizes an over-all advantage of the

theoretically based – and thus widely data-independent – SAFT approaches, whose predictive capabilities are stronger.

3.2. Viscosity measurements

In this study, viscosity measurements of (CO_2 (1) + *n*-pentane (2)) and (CO_2 (1) + *n*-hexane (2)) mixtures were performed at two CO_2 molar compositions (0.1 and 0.3), twelve pressures (from 5 to 100 MPa), and five different temperatures, starting at 293.15 K up to 373.15 K. The experimental viscosities are given in Tables 6 and 7.

Table 6. Experimental viscosities η for (CO_2 (1) + *n*-pentane (2)) mixtures at different conditions of temperature T, pressure p, and CO_2 molar composition x_1. [a]

η / mPa·s					
	T / K				
p / MPa	293.15	313.15	333.15	353.15	373.15
	$x_1 = 0$[b]				
5.00	0.242	0.204	0.173	0.148	0.127
10.00	0.255	0.215	0.184	0.158	0.137
15.00	0.267	0.226	0.194	0.168	0.147
20.00	0.279	0.237	0.204	0.177	0.156
30.00	0.303	0.258	0.223	0.195	0.173
40.00	0.327	0.280	0.242	0.213	0.189
50.00	0.353	0.301	0.262	0.230	0.205
60.00	0.378	0.323	0.281	0.248	0.221
70.00	0.405	0.346	0.301	0.265	0.237
80.00	0.433	0.369	0.321	0.283	0.252

90.00	0.461	0.393	0.341	0.301	0.269
100.00	0.491	0.418	0.362	0.319	0.285
	$x_1 = 0.1000 \pm 0.0017$				
5.00	0.214	0.176	0.148	0.125	0.104
10.00	0.224	0.186	0.158	0.136	0.116
15.00	0.233	0.195	0.168	0.145	0.126
20.00	0.246	0.205	0.177	0.155	0.135
30.00	0.268	0.224	0.195	0.174	0.152
40.00	0.297	0.244	0.215	0.189	0.166
50.00	0.326	0.263	0.232	0.207	0.182
60.00	0.346	0.284	0.249	0.220	0.196
70.00	0.363	0.303	0.269	0.236	0.212
80.00	0.391	0.322	0.282	0.253	0.227
90.00	0.416	0.342	0.299	0.267	0.240
100.00	0.433	0.363	0.318	0.282	0.256
	$x_1 = 0.3003 \pm 0.0026$				
5.00	0.176	0.147	0.124	0.102	
10.00	0.187	0.157	0.134	0.115	0.095
15.00	0.197	0.167	0.143	0.125	0.105
20.00	0.207	0.177	0.153	0.133	0.114
30.00	0.226	0.195	0.170	0.150	0.131
40.00	0.246	0.212	0.187	0.164	0.146
50.00	0.265	0.229	0.202	0.179	0.159
60.00	0.284	0.246	0.218	0.192	0.173
70.00	0.303	0.262	0.232	0.207	0.185
80.00	0.323	0.278	0.248	0.222	0.198

90.00	0.341	0.295	0.263	0.235	0.212
100.00	0.359	0.312	0.277	0.247	0.225

[a] Expanded uncertainties ($k = 2$): $U(T) = 0.02$ K; $U_r(p) = 0.0002$; and $U_r(\eta) = 0.016$

[b] Calculated using REFPROP [21,23].

Table 7. Experimental viscosities η for (CO_2 (1) + *n*-hexane (2)) mixtures at different conditions of temperature T pressure p, and CO_2 molar composition x_1. [a]

η / mPa·s					
	T / K				
p / MPa	293.15	313.15	333.15	353.15	373.15
	$x_1 = 0$[b]				
5.00	0.330	0.273	0.229	0.195	0.167
10.00	0.346	0.288	0.243	0.207	0.178
15.00	0.363	0.302	0.256	0.219	0.190
20.00	0.379	0.316	0.268	0.231	0.201
30.00	0.412	0.345	0.293	0.253	0.221
40.00	0.445	0.373	0.318	0.276	0.242
50.00	0.479	0.401	0.343	0.297	0.261
60.00	0.513	0.430	0.368	0.319	0.281
70.00	0.548	0.459	0.392	0.341	0.300
80.00	0.583	0.488	0.418	0.363	0.320
90.00	0.619	0.518	0.443	0.385	0.339
100.00	0.656	0.549	0.469	0.407	0.359
	$x_1 = 0.1004 \pm 0.0017$				
5.00	0.300	0.247	0.208	0.183	0.159
10.00	0.318	0.261	0.221	0.194	0.168
15.00	0.335	0.275	0.233	0.204	0.176
20.00	0.352	0.288	0.245	0.216	0.186
30.00	0.384	0.315	0.269	0.238	0.206
40.00	0.415	0.342	0.292	0.258	0.228
50.00	0.449	0.371	0.318	0.280	0.249

60.00	0.477	0.398	0.342	0.299	0.267
70.00	0.510	0.425	0.365	0.320	0.285
80.00	0.548	0.453	0.390	0.340	0.304
90.00	0.583	0.490	0.413	0.363	0.323
100.00	0.618	0.516	0.441	0.389	0.355
	$x_1 = 0.3002 \pm 0.0026$				
5.00	0.244	0.203	0.174	0.147	0.122
10.00	0.257	0.216	0.185	0.159	0.134
15.00	0.271	0.230	0.195	0.169	0.146
20.00	0.284	0.241	0.206	0.179	0.156
30.00	0.311	0.263	0.228	0.196	0.174
40.00	0.337	0.287	0.248	0.216	0.191
50.00	0.363	0.310	0.269	0.235	0.207
60.00	0.392	0.332	0.290	0.254	0.225
70.00	0.418	0.356	0.311	0.271	0.242
80.00	0.449	0.378	0.329	0.289	0.260
90.00	0.478	0.398	0.352	0.307	0.275
100.00	0.507	0.420	0.364	0.324	0.293

[a] Expanded uncertainties ($k = 2$): $U(T) = 0.02$ K; $U_r(p) = 0.0002$; and $U_r(\eta) = 0.016$

[b] Calculated using REFPROP [21,22].

As expected, viscosities of the blend (CO_2 + hydrocarbon) monotonically decrease when temperature and molar fraction of CO_2 and they increase with pressure. At the same time, viscosities are significantly enhanced at higher pressures.

In the case of the system (CO_2 (1) + *n*-hexane (2)), the viscosity decreases over the entire range of temperature (293.15 K to 373.15 K) investigated by an average of 46% (ranging from 45%

to 49%), of 45 % (ranging from 43 % to 47 %) and of 44 % (ranging from 42 % to 50 %) for a CO_2 molar composition of x_1 =0; 0.1 and 0.3, respectively. The highest decrease was observed at 5 MPa. Furthermore, the effect of pressure variation (from 5 to 100 MPa) increases the viscosity between 106 % and 123 % at x_1 = 0.1 and between 108 % and 140 % at x_1 = 0.3, whereas, for the pure hexane, it is increased between 99% and 115%. The highest increase was obtained at 373.15 K. Looking at another variable, the viscosity decreases with CO_2 loading (from x_1 = 0.1 to 0.3) by about 17 % for the entire range of pressures and temperatures.

For the other system studied, (CO_2 (1) + *n*-pentane (2)), the behavior is quite similar to the previous one. Viscosity diminishes as function of temperature (from 293.15 K to 373.15 K) between 48 % (at 5 MPa) and 42 % (at 100 MPa) for the pure pentane, between 51 % (at 5 MPa) and 41 % (at 100 MPa) for the mixture with x_1 = 0.1 and between 49 % (at 10 MPa) and 37 % (at 100 MPa) for the mixture with x_1 = 0.3 in the range of pressure from 5 MPa to 100 MPa. Moreover, when the pressure is increased from 5 MPa to 100 MPa, the mixture of x_1 = 0.1 increases its viscosity by 102 % at 293.15 K up to 146 % at 373.15 K and the mixture of x_1 = 0.3 by 104 % (at 293.15 K) up to 142 % (at 353.15 K) whereas, for the pure pentane, the increase is between 103% at 293.15 K and 115% at 373.15 K. Finally, the viscosity decreases by an average of 14 % when the molar composition of CO_2 is increased from 0.1 to 0.3 in the entire range of pressures and temperatures. Experimental data are presented in Figures 4 and 5 for both binary systems where the effects of temperature, pressure, and composition on the viscosity are visualized.

a) b)

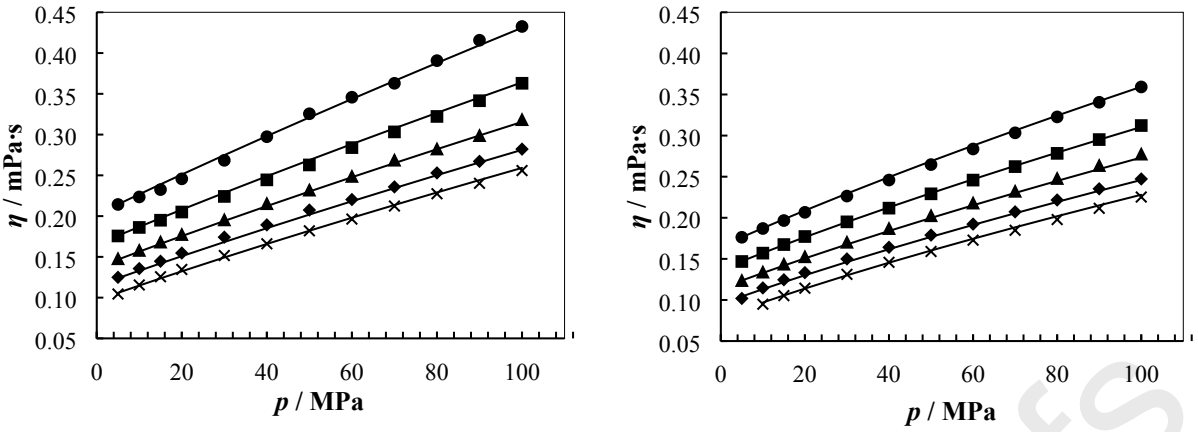

Figure 4. Experimental viscosities of the system (CO_2 (1) + *n*-pentane (2)) at: a) x_1 = 0.1 and b) x_1 = 0.3 as function of pressure at different temperatures: (●) 293.15 K; (■) 313.15 K; (▲) 333.15 K; (♦) 353.15 K; (×) 373.15 K. The lines represent the calculated values using the modified VFT model with the parameters given in Table 8.

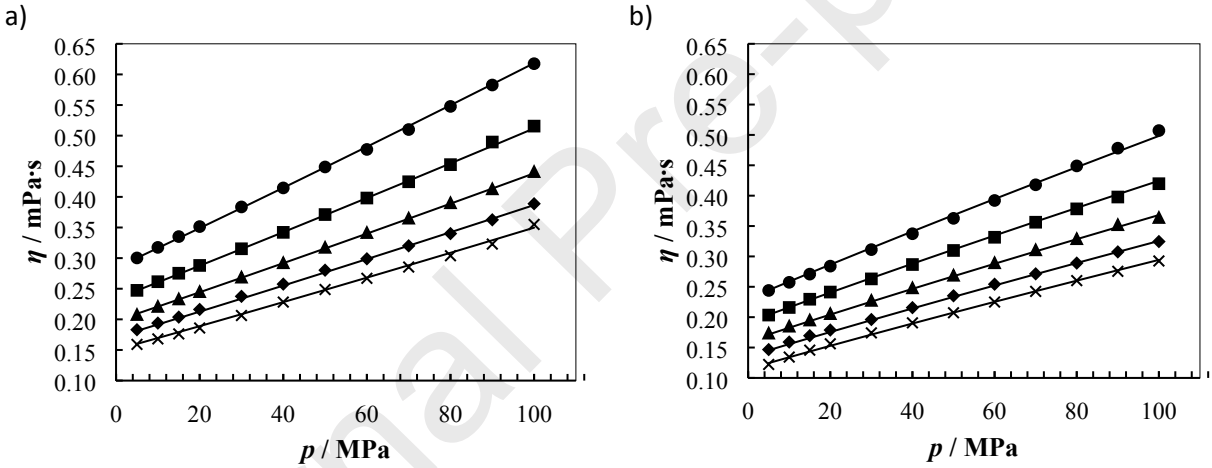

Figure 5. Experimental viscosities of the system (CO_2 (1) + *n*-hexane (2)) at: a) x_1 = 0.1 and b) x_1 = 0.3 as function of pressure at different temperatures: (●) 293.15 K; (■) 313.15 K; (▲) 333.15 K; (♦) 353.15 K; (×) 373.15 K. The lines represent the calculated values using the modified VFT model with the parameters given in Table 8.

The experimental viscosity data were correlated using the modified Vogel-Fulcher-Tammann (VFT) model, Eq (8), an approach that was successfully used by other authors [36,37].

$$\eta(T,p) = A \cdot \exp\left(\frac{B}{T-C}\right) \cdot \left(\frac{p + E(T)}{p_{\text{ref}} + E(T)}\right)^{f} \qquad (8)$$

With $E(T) = E_0 + E_1 \cdot T + E_2 \cdot T^2$

Fitting of the experimental viscosity data was performed applying the least-squares method using the Solver tool of Microsoft Excel software. The fitting results are given in Table 8 which contains the parameters, the standard deviation of the adjustment, and other statistical data. The average absolute deviation *AAD* is within the uncertainty of the experimental viscosities (except for the mixture CO_2 + *n*-pentane with a mole fraction of CO_2 = 0.1) which supports that the model is suitable to be applied for this type of mixtures.

Table 8. Fitting parameters of Eq. (8), standard deviation σ, average absolute deviation *AAD*, and maximum absolute deviation *MAD* for the viscosity measurements.

	CO_2 (1) + *n*-pentane (2)		CO_2 (1) + *n*-hexane (2)	
	x_1 = 0.1	x_1 = 0.3	x_1 = 0.1	x_1 = 0.3
A / mPa·s	0.00132	0.000066	0.02592	0.000168
B / K	2533.126	7042.939	565.816	5696.005
C / K	-204.157	-592.199	62.175	-489.216
E_0 / MPa	-0.04324	-0.00992	-0.04324	-0.04324
E_1 / MPa·K^{-1}	0.62579	0.53863	0.70436	0.61323
E_2 / MPa·K^{-2}	-0.00137	-0.00122	-0.00126	-0.00127
f	0.82157	0.73161	1.10705	0.87236
σ / mPa·s	0.003	0.002	0.003	0.002
AAD / %	1.2	1.0	0.6	0.8
MAD / %	2.8	2.5	1.9	2.3
RMS / %	1.4	1.2	0.8	0.8
p_{ref} / MPa	5	10	5	5

One of the objectives of this work is quantifying the viscosity decrease of the pure hydrocarbon upon the addition of CO_2. For this purpose, a direct comparison was executed. As a result, the

viscosity of *n*-pentane [23,38] decreases between 8 % up to 18 % with the addition of CO_2 starting with pure *n*-pentane up to $x_1 = 0.1$ and between 21 % up to 31 % ending up with $x_1 = 0.3$, respectively. In a similar comparison for the case of pure *n*-hexane [22], the viscosity decreases between 1 % up to 9 % at $x_1 = 0.1$ and between 18 % up to 27 % at $x_1 = 0.3$. Unfortunately, literature data for both binary mixtures are very limited. Kian et al. [12] only measured the viscosity of (CO_2 + *n*-hexane) system at saturation conditions which is far from the *p*, *T*-conditions of our experiments at single-phase homogeneous conditions, thus making a comparison impossible.

The new viscosity data provides an opportunity to examine an accuracy of the modelling framework coupling the entirely predictive Modified Yarranton-Satyro correlation (MYS) with the CP-PC-SAFT EoS [39]. This approach aims at raw estimating the unavailable viscosity data of pure non-associative compounds and their mixtures in wide range of conditions, while MYS employs the molecular parameters of CP-PC-SAFT. In this respect it should be emphasized that the sophisticated nature of viscosity data and their strong pressure and temperature dependencies hinder development of accurate and entirely predictive models whose application does not require any input of experimental data. Despite that, the accuracy of CP-PC-SAFT+MYS approach can at times be comparable to models whose parameters are fitted to the viscosity data. In particular, Thol and Richter [40] have applied REFPROP 8 [41], two recent entropy scaling approaches [42,43] and the *f*-theory model [44] for estimating 12 experimental viscosity points of saturated liquid phase in CO_2 – *n*-hexane reported by Kian and Scurto [12]. These authors reported the AAD values of the considered approaches varying from 9 % to 19 %. The AAD from these data yielded by CP-PC-SAFT+MYS is 12.2 %. Besides that, Thol and Richter [40] obtained AAD varying from 2.2 % to 17 % for 4 points reported by Koller et al. [45]. In the case of CP-PC-SAFT+MYS the AAD% is 13.3 %.

Table 10 compares the predictions of CP-PC-SAFT+MYS for the current viscosity data with the REFPROP 10 Software [21]. As seen, although the results of REFPROP 10 are better, they also exhibit remarkable deviations from the data. In this respect, it should be emphasized that unlike CP-PC-SAFT+MYS REFPROP 10 is based on the existing experimental data. Besides that, it can be seen that the accuracies of both models deteriorate with an increase of x_1 and they perform better in a case of the *n*-pentane system. Remarkable, the high-temperature region has a major contribution to the deviations of CP-PC-SAFT+MYS, which can be explained by inaccuracy of this model in predicting the pertinent pure compound data. Obviously, such shortcomings can be characteristic the entirely predictive approaches.

Table 9. Statistical analysis of deviations from the current viscosity data of REFPROP 10 and CP-PC-SAFT+MYS.

		CO_2 (1) + *n*-pentane (2)		CO_2 (1) + *n*-hexane (2)	
	x_1	0.1	0.3	0.1	0.3
AAD / %	REFPROP 10	5.7	5.8	2.9	12.2
	CP-PC-SAFT+MYS	11.2	24.0	12.8	25.6
BIAS / %	REFPROP 10	5.7	5.8	2.7	12.2
	CP-PC-SAFT+MYS	–11.2	–24.0	–12.8	–25.6
RMS / %	REFPROP 10	1.9	1.5	1.9	2.7
	CP-PC-SAFT+MYS	10.8	14.0	11.5	13.4
MAD / %	REFPROP 10	10.7	8.8	6.1	18.0
	CP-PC-SAFT+MYS	20.8	30.8	24.2	31.8

4. Conclusions

Experimental density and viscosity data of (CO_2 + hydrocarbon) binary mixtures (the hydrocarbons being *n*-pentane and *n*-hexane) were obtained at six molar compositions of CO_2

(0, 0.1, 0.2, 0.3, 0.4, and 0.6) and two molar compositions of CO_2 (0.1 and 0.3) for viscosity. Both mixtures were measured in a wide range of pressure (up to 100 MPa) and temperature. The modified Tammann-Tait equation can fit the density data with standard deviations that in most cases remain within the uncertainty of the measurements. The viscosity data were successfully correlated using a modified VFT model.

In the theoretical part of this work the over-all robustness and reliability of two molecularly based approaches, namely PC-SAFT and CP-PC-SAFT in estimating data of CO_2 – *n*-alkane series were examined. It was found that each of them has its advantages and disadvantages in modelling phase equilibria and excess enthalpies. Despite an obvious superiority of CP-PC-SAFT in predicting speeds of sound, this model is usually slightly inferior in estimating the single-phase densities of the considered systems up to 130 MPa. Such tendency was observed also in a case of the current density data. Although both approaches yielded reasonably good predictions, PC-SAFT was found somewhat more accurate. In addition, performance of the GERG-2008 equation in estimating the densities was considered. This model also yielded nearly precise estimations of CO_2 + *n*-pentane and pure *n*-hexane. However, it was found that addition of CO_2 to *n*-hexane results in a progressive deterioration of its accuracy. Unlike that, both SAFT approaches yielded reasonably good results for this system in the entire composition range. These results emphasize the need of upgrading the GERG-2008 EoS with new accurate experimental data.

The results of an entirely predictive CP-PC-SAFT+MYS modelling framework and the REFPROP 10 Software for the current viscosity data were also examined. Unsurprisingly, the accuracy of REFPROP 10 was superior. However, it was found that both models exhibit remarkable deviations from the data, which increase with addition of CO_2.

Acknowledgments

This research was funded by European Regional Development Fund and the Regional Government of Castilla y León project VA280P18. DVM is funded by the Spanish Ministry of Science, Innovation and Universities ("Beatriz Galindo Senior" fellowship BEAGAL18/00259).

References

[1] Enhanced Oil Recovery | Department of Energy, (n.d.). https://www.energy.gov/fe/science-innovation/oil-gas-research/enhanced-oil-recovery (accessed July 13, 2020).

[2] Carbon Dioxide Enhanced Oil Recovery Untapped Domestic Energy Supply and Long Term Carbon Storage Solution, Pittsburgh, PA, 2010. www.netl.doe.gov (accessed July 13, 2020).

[3] Y. Sanchez-Vicente, W.J. Tay, S.Z. Al Ghafri, J.P.M. Trusler, Thermodynamics of carbon dioxide-hydrocarbon systems, Appl. Energy. 220 (2018) 629–642. https://doi.org/10.1016/j.apenergy.2018.03.136.

[4] G. Cooney, J. Littlefield, J. Marriott, T.J. Skone, Evaluating the Climate Benefits of CO2-Enhanced Oil Recovery Using Life Cycle Analysis, Environ. Sci. Technol. 49 (2015) 7491–7500. https://doi.org/10.1021/acs.est.5b00700.

[5] J. Zambrano, F. V Gómez-Soto, D. Lozano-Martín, M.C. Martín, J.J. Segovia, Volumetric behaviour of (carbon dioxide+hydrocarbon) mixtures at high pressures, J. Supercrit. Fluids. 110 (2016) 103–109. https://doi.org/10.1016/j.supflu.2016.01.002.

[6] G.J. Besserer, D.B. Robinson, Equilibrium-Phase Properties of n-Pentane-Carbon Dioxide System, J. Chem. Eng. Data. 18 (1973) 416–419. https://doi.org/10.1021/je60059a020.

[7] E. Kiran, H. Pöhler, Y. Xiong, Volumetric properties of pentane + carbon dioxide at high pressures, J. Chem. Eng. Data. 41 (1996) 158–165. https://doi.org/10.1021/je9501503.

[8] J. Chen, W. Wu, B. Han, L. Gao, T. Mu, Z. Liu, T. Jiang, J. Du, Phase Behavior, Densities, and Isothermal Compressibility of CO_2 + Pentane and CO_2 + Acetone Systems in Various Phase Regions, J. Chem. Eng. Data. 48 (2003) 1544–1548. https://doi.org/10.1021/je034087q.

[9] G.I. Kaminishi, C. Yokoyama, T. Shinji, Vapor pressures of binary mixtures of carbon dioxide with benzene, n-hexane and cyclohexane up to 7 MPa, Fluid Phase Equilib. 34 (1987) 83–99. https://doi.org/10.1016/0378-3812(87)85052-5.

[10] W.K. Tolley, R.M. Izatt, J.L. Oscarson, Simultaneous measurement of excess enthalpies and solution densities in a flow calorimeter, Thermochim. Acta. 181 (1991) 127–141. https://doi.org/10.1016/0040-6031(91)80418-I.

[11] B. Wang, J. He, D. Sun, R. Zhang, B. Han, Solubility of chlorobutane, ethyl methacrylate and trifluoroethyl acrylate in supercritical carbon dioxide, Fluid Phase Equilib. 239 (2006) 63–68. https://doi.org/10.1016/j.fluid.2005.10.023.

[12] K. Kian, A.M. Scurto, Viscosity of compressed CO_2-saturated n-alkanes: CO_2/n-hexane, CO_2/n-decane, and CO_2/n-tetradecane, J. Supercrit. Fluids. 133 (2018) 411–420. https://doi.org/10.1016/j.supflu.2017.10.030.

[13] J.J. Segovia, O. Fandiño, E.R. López, L. Lugo, M. Carmen Martín, J. Fernández, Automated densimetric system: Measurements and uncertainties for compressed fluids, J. Chem. Thermodyn. 41 (2009) 632–638. https://doi.org/10.1016/j.jct.2008.12.020.

[14] R. Helsel, Visual Programming With HP-VEE, 3rd ed., Prentice Hall PTR, New Jersey, 1998.

[15] Evaluation of measurement data - Guide to the expression of uncertainty in measurement. JCGM 2008., Eval. Meas. Data - Guid. to Expr. Uncertain. Meas. JCGM

2008. (n.d.).

[16] J.R. Zambrano, M. Sobrino, M.C. Martín, M.A. Villamañán, C.R. Chamorro, J.J. Segovia, Contributing to accurate high pressure viscosity measurements: Vibrating wire viscometer and falling body viscometer techniques, J. Chem. Thermodyn. 96 (2016) 104–116. https://doi.org/10.1016/j.jct.2015.12.021.

[17] J. Zambrano, M.C. Martín, Á. Martín, J.J. Segovia, Viscosities of binary mixtures containing 1-butanol+2,2,4-trimethylpentane or+1,2,4-trimethylbenzene at high pressures for the thermophysical characterization of biofuels, J. Chem. Thermodyn. 102 (2016) 140–146. https://doi.org/10.1016/j.jct.2016.07.008.

[18] J. Zambrano, M.C. Martín, A. Moreau, E.I. Concepción, J.J. Segovia, Viscosities of binary mixtures containing 2-butanol + hydrocarbons (2,2,4-trimethylpentane or 1,2,4-trimethylbenzene) at high pressures for the implementation of second generation biofuels, J. Chem. Thermodyn. 125 (2018) 180–185. https://doi.org/10.1016/j.jct.2018.05.027.

[19] M.J. Assael, C.P. Oliveira, M. Papadaki, W.A. Wakeham, Vibrating-wire viscometers for liquids at high pressures, Int. J. Thermophys. 13 (1992) 593–615. https://doi.org/10.1007/BF00501943.

[20] F. Peleties, J.P.M. Trusler, Viscosity of liquid di-isodecyl phthalate at temperatures between (274 and 373) K and at pressures up to 140 MPa, J. Chem. Eng. Data. 56 (2011) 2236–2241. https://doi.org/10.1021/je101256z.

[21] E.W. Lemmon, M.L. Huber, M.O. McLinden, NIST Standard Reference Database 23: Reference Fluid Thermodynamic and Transport Properties (REFPROP), Version 10.0, Phys. Chem. Prop. (2018) 135. https://doi.org//10.18434/T4/1502528.

[22] R. Thol, M; Wang, Y; Lemmon, E.W.; Span, Fundamental Equations of State for Hydrocarbons. Part II. n-Hexane, To Be Publ. (n.d.).

[23] R. Thol, M.; Uhde, T.; Lemmon, E.W.; Span, Fundamental Equations of State for Hydrocarbons. Part I. n-Pentane, To Be Publ. (n.d.).

[24] R. Span, W. Wagner, A new equation of state for carbon dioxide covering the fluid region from the triple-point temperature to 1100 K at pressures up to 800 MPa, J. Phys. Chem. Ref. Data. 25 (1996) 1509–1596. https://doi.org/10.1063/1.555991.

[25] F. Audonnet, A.A.H. Pádua, Simultaneous measurement of density and viscosity of n-pentane from 298 to 383 K and up to 100 MPa using a vibrating-wire instrument, Fluid Phase Equilib. 181 (2001) 147–161. https://doi.org/10.1016/S0378-3812(01)00487-3.

[26] T. Regueira, W. Yan, E.H. Stenby, Densities of the binary systems n-hexane + n-decane and n-hexane + n-hexadecane up to 60 MPa and 463 K, J. Chem. Eng. Data. 60 (2015) 3631–3645. https://doi.org/10.1021/acs.jced.5b00613.

[27] J. Zhou, R. Zhu, H. Xu, Y. Tian, Densities, excess molar volume, isothermal compressibility, and isobaric expansivity of (dimethyl carbonate+n-hexane) systems at temperatures (293.15 to 313.15)K and pressures from 0.1MPa up to 40MPa, J. Chem. Thermodyn. 42 (2010) 1429–1434. https://doi.org/10.1016/j.jct.2010.06.011.

[28] L.E. Camacho-Camacho, L.A. Galicia-Luna, Experimental Densities of Hexane + Benzothiophene Mixtures from (313 to 363) K and up to 20 MPa, J. Chem. Eng. Data. 52 (2007) 2455–2461. https://doi.org/10.1021/je7003929.

[29] J. Gross, G. Sadowski, Perturbed-Chain SAFT: An Equation of State Based on a Perturbation Theory for Chain Molecules, Ind. Eng. Chem. Res. 40 (2001) 1244–1260. https://doi.org/10.1021/ie0003887.

[30] I. Polishuk, Standardized Critical Point-Based Numerical Solution of Statistical Association Fluid Theory Parameters: The Perturbed Chain-Statistical Association Fluid Theory Equation of State Revisited, Ind. Eng. Chem. Res. 53 (2014) 14127–14141. https://doi.org/10.1021/ie502633e.

[31] O. Kunz, R. Klimeck, W. Wagner, M. Jaeschke, GERG Technical Monograph 15 (2007) The GERG-2004 wide-range equation of state for natural gases and other mixtures, 2007.

[32] O. Kunz, W. Wagner, The GERG-2008 Wide-Range Equation of State for Natural Gases and Other Mixtures: An Expansion of GERG-2004, J. Chem. Eng. Data. 57 (2012) 3032–3091. https://doi.org/10.1021/je300655b.

[33] J. García, L. Lugo, J. Fernández, Phase Equilibria, PVT Behavior, and Critical Phenomena in Carbon Dioxide + n-Alkane Mixtures Using the Perturbed-Chain Statistical Associating Fluid Theory Approach, Ind. Eng. Chem. Res. 43 (2004) 8345–8353. https://doi.org/10.1021/ie049691o.

[34] C. Zhao, D. Lu, K. Chen, Y. Chi, S. Liu, L. Yuan, Y. Zhang, Y. Song, Review of Density Measurements and Predictions of CO_2–Alkane Solutions for Enhancing Oil Recovery, Energy & Fuels. 35 (2021) 2914–2935. https://doi.org/10.1021/acs.energyfuels.0c03914.

[35] J.M. Garrido, I. Polishuk, Toward Development of a Universal CP-PC-SAFT-Based Modeling Framework for Predicting Thermophysical Properties at Reservoir Conditions: Inclusion of Surface Tensions, Ind. Eng. Chem. Res. 57 (2018) 8819–8831. https://doi.org/10.1021/acs.iecr.8b02091.

[36] M.J.P. Comuñas, A. Baylaucq, C. Boned, J. Fernández, High-Pressure Measurements of the Viscosity and Density of Two Polyethers and Two Dialkyl Carbonates, Int. J. Thermophys. 22 (2001) 749–768. https://doi.org/10.1023/A:1010770831215.

[37] X. Paredes, O. Fandiño, A.S. Pensado, M.J.P. Comuñas, J. Fernández, Experimental density and viscosity measurements of di(2ethylhexyl)sebacate at high pressure, J. Chem. Thermodyn. 44 (2012) 38–43. https://doi.org/10.1016/j.jct.2011.07.005.

[38] J. Zambrano, Desarrollo De Un Viscosímetro De Hilo Alta Presión De Nuevos Biocombustibles, Universidad de Valladolid, 2014.

[39] I. Polishuk, A Modeling Framework for Predicting and Correlating Viscosities of Liquids in Wide Range of Conditions, Ind. Eng. Chem. Res. 54 (2015) 6999–7003. https://doi.org/10.1021/acs.iecr.5b01468.

[40] M. Thol, M. Richter, Dynamic Viscosity of Binary Fluid Mixtures: A Review Focusing on Asymmetric Mixtures, Springer US, 2021. https://doi.org/10.1007/s10765-021-02905-x.

[41] J.C. Chichester, M.L. Huber, Documentation and assessment of the transport property model for mixtures implemented in NIST REFPROP (version 8.0), Gaithersburg, MD, 2008. https://doi.org/10.6028/NIST.IR.6650.

[42] J. Mairhofer, A Residual Entropy Scaling Approach for Viscosity Based on the GERG-2008 Equation of State, Ind. Eng. Chem. Res. 60 (2021) 2652–2662. https://doi.org/10.1021/acs.iecr.0c04938.

[43] X. Yang, X. Xiao, E.F. May, I.H. Bell, Entropy Scaling of Viscosity—III: Application to Refrigerants and Their Mixtures, J. Chem. Eng. Data. 66 (2021) 1385–1398. https://doi.org/10.1021/acs.jced.0c01009.

[44] S.E. Quiñones-Cisneros, C.K. Zéberg-Mikkelsen, A. Baylaucq, C. Boned, Viscosity Modeling and Prediction of Reservoir Fluids: From Natural Gas to Heavy Oils, Int. J. Thermophys. 25 (2004) 1353–1366. https://doi.org/10.1007/s10765-004-5743-z.

[45] T.M. Koller, S. Yan, C. Steininger, T. Klein, A.P. Fröba, Interfacial Tension and Liquid Viscosity of Binary Mixtures of n-Hexane, n-Decane, or 1-Hexanol with Carbon Dioxide by Molecular Dynamics Simulations and Surface Light Scattering, Int. J. Thermophys. 40 (2019). https://doi.org/10.1007/s10765-019-2544-y.

Highlights

Density and viscosity behavior of CO_2 + pentane or hexane is determined.

Measurements were carried out up to 100 MPa and temperatures (293.15 to 393.15) K.

The data were good correlated using Tammann-Tait and VFT models for densities and viscosities, respectively.

GERG 2008, PC-SAFT and CP-PC-SAFT are examined for modelling densities.

Viscosities were compared with REFPROP10 and MYS+ CP-PC-SAFT predictions.

Author statement

Alejandro Moreau: Investigation, Validation, Formal analysis, Writing – Original Draft

Ilya Polishuk: Conceptualization, Formal Analysis, Writing - Review & Editing

José J. Segovia: Conceptualization, Methodology, Validation, Supervision

Dirk Tuma: Writing - Review & Editing

David Vega-Maza: Validation, Formal Analysis

M. Carmen Martín: Supervision, Writing - Review & Editing, Project administration, Funding acquisition

Declaration of interests

☒ The authors declare that they have no known competing financial interests or personal relationships that could have appeared to influence the work reported in this paper.

☐The authors declare the following financial interests/personal relationships which may be considered as potential competing interests: